Oil detection algorithm based on edge detection

MA Teng-bo[1,2,3], WANG Si-yuan[4]

1. *Institute of Electronics, Chinese Academy of Sciences, Beijing* 100190, *China*;
2. *Key Laboratory of Spatial Information Processing and Application System Technology, Chinese Academy of Sciences, Beijing* 100190, *China*;
3. *Graduate University of Chinese Academy of Science, Beijing* 100049, *China*;
4. *Center for Earth Observation and Digital Earth, Chinese Academy of Sciences, Beijing* 100190, *China*

Abstract: The side-look imaging of SAR (Synthetic Aperture Radar) may result in the pockety density, so we can not get a satisfying result by using CFAR (constant false alarm rate) detection on the whole image. To improve the oil detection capability, we propose a new oil detection method based on edge detection in this paper. First, the AOI (area of interest) of oil is detected through radio edge detection, then an improved Weibull-CFAR detector is applied to the AOI. Comparing with the whole CFAR detection results, this detection method demonstrates better accuracy and efficiency on SAR images with pockety density, especially suitable for the oil detection of big images.

Key words: synthetic aperture radar (SAR), oil detection, constant false alarm rate(CFAR), ratio edge detection (ROA)
CLC number: TP751.1/X55 **Document code:** A

1 INTRODUCTION

With the unceasing exploitation of oil resources, the pollution of oil spill in sea becomes more and more serious day by day. Within all kinds of marine pollution, oil spill pollution, which has seriously impacted people's life, ranks top in terms of occurrence frequency, dispersing area and damage degree. Therefore, how to deal with the oil spill pollution effectively and scientifically has become an important issue, and the precondition to solve the oil spill pollution is how to find an accurate and quick detection method of oil spill.

Since SAR is the all-day and all-weather radar, it becomes the favorite in oil spill detections. These years, the researches on automatic oil spill extraction on the SAR image are rather popular. For example, the method of adaptive threshold detection based on mobile window (Bjerde *et al.*, 1993). This method first determines whether the region in the window is homogeneous. If its histogram shows two peaks then use threshold detection. We can also use gray-scale information or statistical characters to make a pre-segmentation, then use a merger algorithm to detect oil spill (Barni *et al.*, 1995; Chang *et al.*, 2005). In addition, there are also some people acquiring the information extraction by using the region growing method (Araujo *et al.*, 2004). Among these detection methods, the oil spill information extracted by adaptive threshold detection is incomplete, and the information could not be extracted if window is completely filled with oil spills. For method based on merger and segment, it is difficult to determine the judgment criteria, and the process of merger takes too much time, so it does not suit large images. The result of regional growth depends on the selection of seed point. Presently the widely used method is to select the peak of the histogram as seed point, but the characteristic of side-look imaging makes image appear bright in one side but dark in the other side. Therefore, the histogram can not reflect the partial characteristics very well, which makes it difficult to obtain good results. For the above reasons, in this paper we propose a rapid algorithm of oil spill detection, this algorithm combines edge detection and CFAR, fits for big images with non-uniform gray. First it uses the ratio of edge detection (ROA) to monitor the approximate location of film, marking it as AOI by rectangular, then carries on the CFAR detection to the AOI. Experiments show that this algorithm can better fit the background of sea which is not only complex but highly localized in SAR image, and can obtain a better result.

2 METHOD OF OIL SPILL EXTRACTION BASED ON EDGE DETECTION

2.1 Analysis characteristic of oil spill on SAR images

The oil film's thickness on the sea surface changes rapidly. It increases the ocean surface tension and causes the damping effect to wave field. Since this effect will change the backscattering of sea surface, the oil spill can be reflected well in SAR

Received: 2008-05-22; **Accepted**: 2009-01-14
Foundation: Automatic Oil detection based on remote sensing image and application demonstration (No.200705018); National 863 program (No.098004101A)
First author biography: MA Teng-bo(1986—), female, Graduate University of Chinese Academy of Science, signal and information processing, now major in image processing. E-mail: biyanbobo@163.com.

images. The most prominent characteristic of oil film is the damping effect on surface capillary wave and short gravity wave. When the incident angle of radar is between 20°—70°, the scattering of the sea is mainly Bragg scattering. Bragg scattering's short-wave is influenced by damping because of the oil film, thus will change the surface roughness, which is the main factor that impact the sea's backscattering coefficient.

When the sea is covered by oil film, the surface tension waves and short gravity waves will be damped, surface becomes smoother and the surface roughness is decreased, thus reduce the reflex of oil spill in the radar signal, that is, the radar backscattering coefficient of sea's surface is decreased. The gray level of the corresponding parts in SAR images is reduced. That is the reason why the observed oil spills are usually presented as dark spots, patches or stripes in SAR images, and we can take advantage of this characteristic to identify the oil spill region.

2.2 AOI detection based on ROA

2.2.1 ROA edge detection

Because the speckle noise of SAR image is relatively serious, the common method of edge detection cannot obtain good results. Taking into account of this, we use Ratio edge detection algorithm method.

Assuming the size of rectangular sliding window is M×M, when it slides on the image, the center of the window is set to be the detection point. For a straight line L that go through this point along a particular directions, we calculate the respective sample average u_1、u_2 in non-overlapping regions of both side of the window, then average the two samples to get R

$$R=\begin{cases}\dfrac{\min(u_1,u_2)}{\max(u_1,u_2)}, \max(u_1,u_2)!=0\\ 1, \max(u_1,u_2)=0\end{cases} \tag{1}$$

From the calculation of R, it can be seen when R tends to 1, the two regions are more likely to belong to a homogeneous area; instead when R tends to 0, the point is more likely to be on the border of two regions. Considering the different orientation of the edge, we make detection on each point in the four directions shown in Fig.1 (a)—(d) and get the smallest R. The size of window in Fig. 1 is 5×5, it can be adjusted according to situation.

In practice, there is little contrast between sea water and oil spill, their border is not very clear with certain degree of blurring. In Fig. 1(e), pixels adjacent to the target pixel are set to be mask pixels, they are not involved in the calculation of average value, and the number of mask pixels depends on actual situation, so we are able to get the blurring edge.

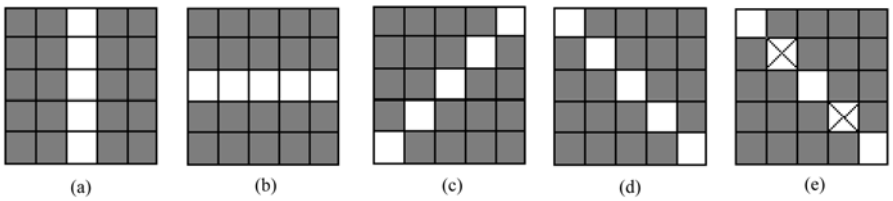

Fig. 1 Structure of ROA operator

(a)Vertical; (b) Horizontal; (c) 45°; (d) 135°; (e) Plus mask

Using a main threshold T to compare with R, when $R<T$, the point is considered as an edge point; while the detection window is in a homogeneous area, if $0<R<T$, which means that there are two heterogeneous regions, then it is an error detection. In the L-look SAR images, the homogeneous region of image obey Gamma distribution:

$$p(I)=\frac{1}{\Gamma(L)}\frac{1}{\sigma^2}\left(\frac{1}{\sigma^2}\right)^{L-1}\exp\left(-\frac{1}{\sigma^2}\right) \tag{2}$$

Under the precondition that the image conforms to Gamma distribution, the error probability P is

$$\begin{aligned}P(T)&=P(R<T\,|\,\text{homogeneity})\\&=\int_0^T f(R\,|\,1)\mathrm{d}R\\&=\int_0^T\frac{\Gamma(2NL)}{\left(\Gamma(NL)\right)^2}R^{NL-1}\frac{2}{(R+1)^{2NL}}\mathrm{d}R\end{aligned} \tag{3}$$

If we ignore the pertinence among tests, it can be considered as four-scale Bernoulli experiment and $P_1\in[0,1]$, the detection process meets the geometric distribution, in this case the error probability of this detection is

$$P_4=1-(1-P_1)^4 \tag{4}$$

From the Eq.(3) and Eq.(4), if taking L=3 as the number of image view, the error probability curve can be drawn as shown in Fig. 2.

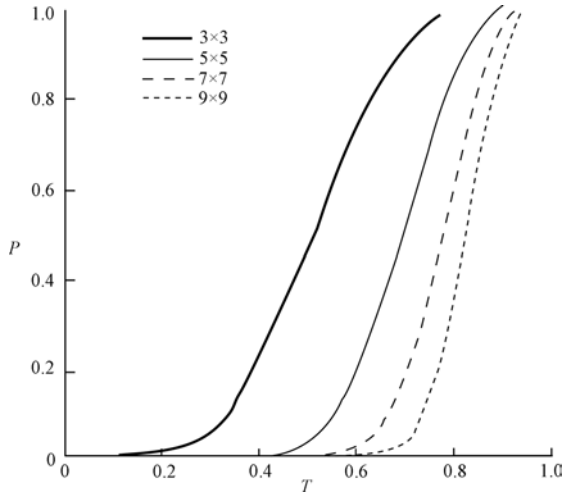

Fig. 2 *P-T* curve of four orientation detection

The error probability of Ratio algorithm are determined merely by the SAR image's look number, the threshold and pixel number in the detection window not the pixel gray value, so it can overcome the problem of uneven grayscale and has a relatively good inhibitory effect to the speckle noise. Ratio algorithm has a constant false alarm probability, can make a very good detection on edge of SAR image, but the larger the detection window is, the wider the edge has, it needs more processing to obtain edge of a single pixel. In this paper, we only needs to get the rough location of oil spill through the edge image, the ROA test results can be directly used in the next phase of AOI extraction, thus greatly simplify the algorithm and reduce the calculating time.

2.2.2 AOI detection

After edge detection, we obtain a binary image of edge information, and we can start the selection of AOI: making a connective region transformation on the edge image, removing the small connective region, adding a rectangle to each connective region and finally formming the initial AOI.

In oil spill images, besides oil film and sea water, there probably exist some islands, ships and other objects, and the edge of these objects are also be found in edge information. Therefore, the initial AOI possibly does not include the oil spill but other objects. This will increase the false alarm rate, so it is necessary to filter these AOIs before going on for further processing.

We adapt a method based on region growth to pre-treat AOI, as follows:

(1) Choosing a gray threshold for the AOI.

(2) In this AOI, finding the first unmarked pixel point which is larger than the chosen threshold in step (1). If the point is found, put it into the stack and mark the pixel, set the counter variable Count=1, if the point is not found, then skip the present steps and deal with the next AOI.

(3) Testing whether the stack is empty, if not, then take the first pixel out of the stack and make a four-connected region detection, putting the unmarked neighborhood pixel which is larger than the chosen threshold into the stack, marking this pixel and increasing the counter variable's value. If the stack is empty, go back to step (2).

(4) If Count>a/5, where a is the area of AOI, then delete the AOI and deal with the next AOI, otherwise return to step (3).

After the process in the previous step, these AOIs will include most information of oil spill, then expand the AOI border to increase the background information, at the same time merging these AOIs, which are relatively near, to obtain final AOIs.

2.3 Improved CFAR detection

CFAR detection plays an important part in automatic target detection of radar images. Its essence is to adjust the false alarm probability to a specific degree according to different backgrounds. The key of CFAR detection is the determination of adaptive threshold value. Assuming that $p(x)$ is the probability density function of radar clutter's distribution model, then $F(x)=\int_0^x p(t)\mathrm{d}t$, where $F(x)$ is an increasing function, we can get the threshold I_c by solving the equation

$$1-P_{\mathrm{fa}}=\int_0^{I_c} p(x)\mathrm{d}x \tag{5}$$

in which the P_{fa} is the false alarm probability.

For a given P_{fa}, we can get the solution of Eq. (5) through dichotomy. Finding a positive integer I to satisfy

$$F(I)\leqslant 1-P_{\mathrm{fa}} \quad \text{and} \quad F(I+1)>1-P_{\mathrm{fa}} \tag{6}$$

then I is the threshold I_c.

From Eq.(5), we can see that estimating the background's distribution model is not only the base of CFAR detection, but also the key of reducing the false alarm. It's generally believed that if using the ocean as background, the clutter usually conforms to k distribution and Weibull distribution model. However, because the gray of oil is lower than the ocean, we need to inverse the image before carrying out the CFAR detection, after this, the gray focus on the high part of grayscale, so its clutter model will change. We select the Weibull distribution as clutter model after testing.

The probability density function of Weibull distribution is

$$p(x)=\begin{cases}\dfrac{c}{b}\left(\dfrac{x}{b}\right)^{c-1}\exp\left[-\left(\dfrac{x}{b}\right)^{c}\right], x\geqslant 0\\ 0, x<0\end{cases} \tag{7}$$

where b is the scale parameter while c is the shape parameter. When c=2, the Weibull distribution degenerate to the Rayleigh distribution, and to exponential distribution when c=1.

Using the model mentioned above, we define a partial window for each AOI, so that each AOI is divided into protective part and background part (as shown in Fig. 3). We use background window to make the background clutter statistics, the protective window is designed to prevent the target pixel from leaking to background, which will affect the correctness of background clutter's statistic. We select the size of protective window based on experiences, while in this paper its length and width are set to 3/5 of the AOI's.

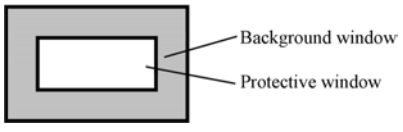

Fig. 3 Structure of window

Using the character of Weibull distribution and the data of the background window, we can get the scale parameter and shape parameter through the relationship between one-order moments and second-order moments.

The first-order moments and the second-order moments of the Weibull distribution are as follow:

$$E[x]=\int_{-\infty}^{+\infty} xP(x)\mathrm{d}x=b\Gamma\left(1+\frac{1}{c}\right) \tag{8}$$

$$E[x^2]=\int_{-\infty}^{+\infty} x^2P(x)\mathrm{d}x=b^2\Gamma\left(1+\frac{2}{c}\right) \tag{9}$$

We define

$$R=\frac{E[x^2]}{\left(E[x]\right)^2}=\frac{\Gamma\left(1+\frac{2}{c}\right)}{\left[\Gamma\left(1+\frac{1}{c}\right)\right]^2} \tag{10}$$

One of the best polynomial curve fitting for the function above is $c=\frac{a_2}{R-1}+\frac{a_1}{\sqrt{R-1}}+a_0$, in which the parameters a_2=0.0791, a_1=0.8481, a_0=0.0817.

Thus the scale parameter of Weibull distribution $b=\frac{E[x]}{\Gamma\left(1+\frac{1}{c}\right)}$, taking the value of b and c into Eq. (6) and Eq. (7), we can obtain the threshold.

2.4 Post-processing

In target detection we use CFAR detection，it deals with the pixel, the speckle noise of SAR image make the target be much likely to become multiply connected regions. In addition, the oil spill's edge is finely-broken，this will make the perimeter be longer. In order to improve the accuracy of results, it is necessary to carry out post-processing to obtain more precise information. In this paper, we mainly use morphology and boundary tracking algorithm.

3 ANALYSIS OF TEST RESULT

Using the above-mentioned algorithm, we conduct a preliminary study on oil spill image in Bohai Sea area. In this paper, all images used in the experiment are Envisat images of Bohai region. Taking into account that there may be distribution differences existing between the overall background and local background, we select the false alarm rate through experimental comparison.

In Fig. 4(a), the size of image which is acquired in January 2007 is 4560×4128.We can see scaly corrugation caused by wind or other factors, while the whole gray scale has shown the uneven distribution because of side-look imaging.

Fig. 4(b) is the result of overall CFAR test. Experiments show that when the false alarm rate is 0.03, the test results are relatively satisfactory. But due to the using of main threshold, the corrugation which is relatively dark in the centre of image is also detected as oil spills. There exist many false alarms, while the oil spill in the marked rectangle is not detected completely.

Fig. 4(c) is the result of the algorithm by applying the method indicated in this paper. The size of detective window in ROA edge detection is 9×9. Because the gray of the corrugation changes slowly in the image, if the mask window's size is set too large, it will make the corrugation be detected as AOI. We take 3×3 as the size, namely, one mask pixel on each four direction of the target pixel. The false alarm rate is set to 0.02 in the part of CFAR detection, the rectangular box is automatically selected as AOI by algorithm. As it can be seen, most of the oil spill can be detected effectively, and the negative impact by the surface wave is also effectively inhibited.

Fig. 5(a) is another oil spill image whose size is 1364×1404, and the acquisition time for the image is September 2007. You can clearly see that there are many vessels whose gray is higher in the image, while the gray of the whole image have also demonstrated a degree of imbalance. Exerting the overall CFAR algorithm and the algorithm mentioned in the text on the image respectively, the false alarm rate is set to 0.1 in the former and the latter 0.12. The results are showed in Fig. 5(b), Fig. 5(c). By contrasting the two figures we can see, the oil spill in the bottom-left corner of the image can be detected well by the algorithm, and the impact brought by vessels in edge detection is effective inhibit.

Fig. 6(a) and Fig. 6(b) are results of CFAR detection without and with protective window respectively. While taking the same false alarm rate (0.12), the detective result in Fig. 6(a) is obviously better than the one in Fig. 6(b), illustrating that the improved CFAR algorithm match the clutter model better. Fig. 6(c) is the result of edge after post-processing, comparing with the edge in Fig. 6(b), the edge of oil spill become smoother, and minor part of the border is inhibited well.

After testing images of different regions, it proves that this algorithm has higher reliability and can achieve more desirable results in practical application.

4 CONCLUSIONS

In this article, we analyze SAR images of oil spill and pro-

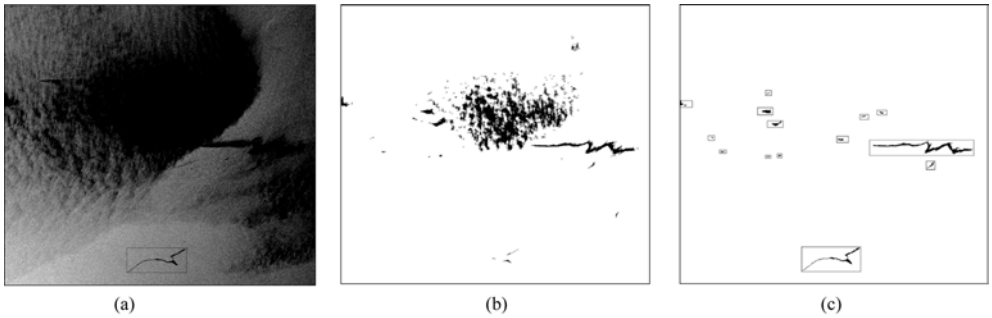

Fig. 4 Envisat image of Bohai and detection results

(a) Original image; (b) Result of whole CFAR detection; (c) Result of the arithmetic mentioned in this paper

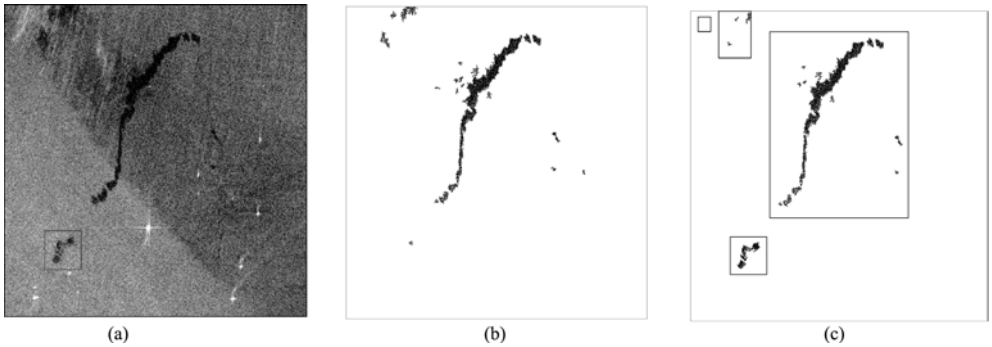

Fig. 5 Envisat image of Bohai and detection results
(a) Original image; (b) Result of whole detection (false alarm 0.1); (c) Result of the arithmetic mentioned in this paper

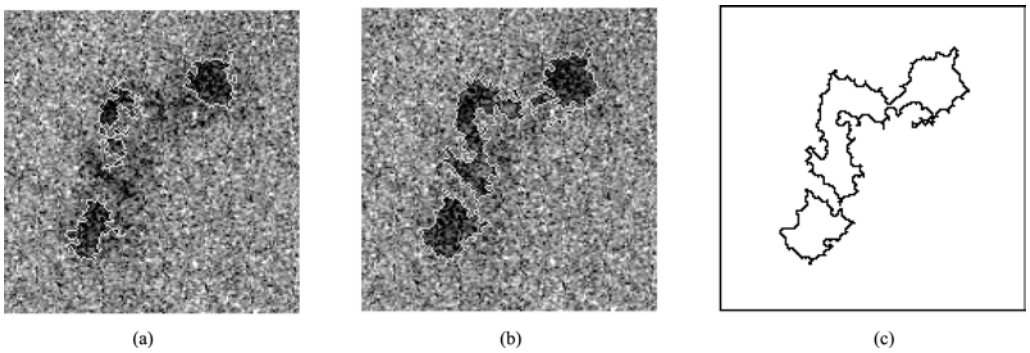

Fig. 6 Improved CAFR detection and result of post-processing
(a) Without protective window; (b) With protective window; (c) Result of post-processing

pose an algorithm based on edge detection for the oil spill extraction. Experimental results show that for the non-uniform gray image, the algorithm proposed in this paper is obviously better than the overall detection, it can effectively detect the target area with lower false alarm. At the same time, because it highlights the target through AOI detection, it deal with the large image with higher timeliness and improve the accuracy of detection. It is also easy to be realized. This algorithm has surely some deficiencies, for example, it's difficult to meet all the AOIs with an equal clutter model and false alarm rate etc. These problems should be further studied and improved in the future.

REFERENCES

Araujo R T S, Medeiros F N S, Costa R C S, Marques R C P, Moreira R B and Silva J L. 2004. Spots segmentation in SAR images for remote sensing of environment. *IEEE Image Analysis and Interpretation*. 95—99

Barni M, Betti M and Mecocci A. 1995. A fuzzy approach to oil spill detection on SAR images. Proc.IGARSS'95. **1**: 157—159

Bjerde K W, Solberg A H S and Solberg R.1993.Oil spill detection in SAR imagery. Proc. IGARSS'93. **3**: 943—945

Chang L, Cheng C M and Tang Z S. 2005. An automatic detection of oil spill in SAR images by using image segmentation approach. Proc. IGARSS'93. 1021—1024

Ganugapati S S and Moloney C R. 1995. A ratio edge detector for speckled images based on maximum strength edge pruning. *IEEE Image Processing*, **2**: 165—168

Li L, Deng F, Peng H L. 2002. CFAR target detection in SAR imagery. *Journal of Test and Measurement Technology*, **16**: 9—13

Lu Y, Sun H, Cao Y F, Wang Q and Xu G. 2003. An improved edge detection algorithm of SAR Images. *Journal of Wuhan University*, **49**(1): 107—111

Migliaccio M, Tranfaglia M and Ermakov S A. 2005. A physical approach for the observation of oil spills in SAR images. *IEEE Journal of Oceanic Engineering*, **30**: 496—507

基于边缘分析的海面溢油检测

马腾波[1,2,3], 王思远[4]

1. 中国科学院 电子学研究所, 北京 100190;
2. 中国科学院 空间信息处理与应用系统技术重点实验室, 北京 100190;
3. 中国科学院 研究生院, 北京 100049;
4. 中国科学院 对地观测与数字地球科学中心, 北京 100190

摘 要: 提出一种基于边缘检测的快速溢油信息提取方法, 首先对溢油图像进行 ROA(radio of average)边缘检测, 根据检测结果进行 AOI(area of interest)提取, 然后使用改进的 Weibull-CFAR 检测算法对 AOI 进行溢油检测, 并与全局 CFAR 检测结果进行对比。实验结果证明, 所提出的方法对于非均匀灰度 SAR 图像溢油检测准确性较好、效率较高, 特别适用于大图像的快速溢油检测。

关键词: 合成孔径雷达(SAR), 溢油检测, 恒虚警率(CFAR), 比率边缘检测(ROA)

中图分类号: TP751.1/X55 文献标识码: A

1 引 言

随着石油资源的不断开发利用, 海洋水体油污染问题日趋严重, 在海洋污染中, 石油污染无论在发生频率、分布广度, 还是在危害程度上均居首位, 对人们的生产生活造成严重危害。科学有效地解决海面溢油污染, 对海面溢油进行准确和快速的识别是非常重要的研究项目。

由于 SAR 图像具备全天时全天候监测的特点, 成为溢油检测的热点, 近年来对 SAR 图像进行自动溢油提取的研究广泛。如基于移动窗的自适应阈值检测的方法(Bjerde 等, 1993), 首先判断窗内是否为同质区域, 若这个区域的直方图呈现双峰, 则对该窗口进行阈值检测, 还可以利用灰度信息或者统计特性将图像进行预分割, 再进行合并的方法来检测溢油(Barni 等, 1995. Chang 等, 2005), 此外, Araujo 等(2004)利用区域生长进行信息提取。在这几种检测方法中, 自适应阈值检测方法检测出的溢油信息不完整, 倘若窗口中全是溢油信息则无法检测出。而基于分割合并的方法, 其难点在于判断准则的选取, 同时在合并过程中需要耗费比较多的时间, 不适合对大图像的处理。区域生长的好坏取决于种子点的选取, 目前应用比较广泛的是利用直方图的峰值点作为种子点, 但是 SAR 侧视成像的特点使得图像一边亮一边暗, 直方图无法很好的反映出局部特点, 难以获得很好的检测结果。鉴于上述原因, 本文提出了一种针对灰度不均匀的大图像进行快速检测溢油的算法, 将边缘检测和 CFAR 相结合, 首先利用比率边缘检测(radio of average, ROA)监测出油膜的大致位置, 并用矩形将其标记为 AOI(area of interest), 然后针对这些 AOI 进行改进的 CFAR 检测。实验表明, 该方法能更好的适应 SAR 图像海面背景复杂且局部性强的情况, 获得了较好的检测结果。

2 基于边缘检测的快速溢油提取方法

2.1 溢油 SAR 图像特征分析

海面上的油膜厚度变化很快, 由于其大分子特性增加了海洋表面的张力, 对海面的波浪场产生阻尼作用, 由于这种作用改变了海面的后向散射特性能够在 SAR 图像上有很好的反映。海洋表面油膜最显著的特点就是它们对海面毛细波和短重力波的阻尼作用, 即表面油膜阻尼海面的短表面波。当雷达波的入射角范围在 20°—70°时, 此时海面散射以

收稿日期: 2008-05-22; 修订日期: 2009-01-14

基金项目: 国家“十一五”海洋公益项目(编号: 200705018)和国家 863 重大项目(编号: 098004101A)。

第一作者简介: 马腾波(1986—), 女, 2006 年毕业于西安电子科技大学测控技术与仪器专业。现为中国科学院电子学研究所硕士研究生, 目前主要从事遥感图像处理方面的研究工作。E-mail: biyanbobo@163.com。

Bragg 散射为主。表面油膜的存在使产生 Bragg 散射的短表面波受到阻尼，改变海面的粗糙度这一影响海洋表面目标后向散射系数的主要因素。

当海面上覆盖一层油膜时，海面张力波和短重力波由于受到阻尼，海面变得更为平滑，海面糙度减小，使得溢油区域在雷达信号波段的反射性降低，即海面的雷达后向散射系数降低，该部分海域对应的 SAR 图像灰度级降低，颜色变暗。这也就是为什么在SAR图像上观察到的海上溢油通常呈现颜色较暗的斑点、斑块或条形状，可以利用这个特征，在 SAR 图像上识别溢油区域。

2.2 基于 ROA 的 AOI 提取

2.2.1 ROA 边缘提取

由于 SAR 图像本身的斑点噪声比较严重，常用的边缘检测方法无法获得比较好的结果。针对 SAR 图像中所特有的相干乘性噪声，应用Ratio算法进行边缘检测。

令矩形滑动窗口的大小为 $M\times M$，其在图像上滑动时，将窗口的中心点设为检测点，对于沿某一特定方向过该点的直线 L，计算窗口内两侧不重叠区域的各自样本均值 u_1、u_2，再求两样本均值的 R

$$R=\begin{cases}\dfrac{\min(u_1,u_2)}{\max(u_1,u_2)}, \max(u_1,u_2)!=0\\ 1, \max(u_1,u_2)=0\end{cases} \tag{1}$$

由 R 的定义可以看到，R 趋于 1，则两区域均值越接近，越可能同属于一块均匀区；反之 R 趋于 0，则两区域差别越大，待测点越可能处于两区域间的边界上。考虑到边缘的不同取向，对每一个点按图 1 中(a)—(d)所示的 4 个方向各做一次检测，保留 R 值最小的结果。图 1 中窗口为 5×5，可根据实际情况调整窗口大小。

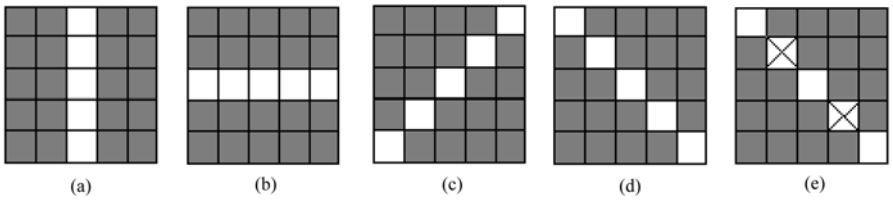

图 1 ROA 算子结构

(a)垂直; (b)水平; (c) 45°; (d) 135°; (e)加掩膜

在实际情况中，海水与溢油的对比度不大，溢油图像上油与水的边界不是很清楚，具有一定的模糊性。在图 1(e)中，将与目标像元相邻的像元设为掩模像元，不参与均值的计算，掩模像元的个数视实际情况而定，这样我们便可以获取模糊边缘。

用一全局阈值 T 与 R 值比较，当 $R<T$ 时即认为该点为边缘点，当检测窗包含于均匀区中时，若 $0<R<T$，则表示有两异质区域存在，此种情况为检测错误。对于 L 视功率 SAR 图像，在均匀区域图像分布服从 Gamma 分布。

$$p(I)=\frac{1}{\Gamma(L)}\frac{1}{\sigma^2}\left(\frac{1}{\sigma^2}\right)^{L-1}\exp\left(-\frac{1}{\sigma^2}\right) \tag{2}$$

在图像满足 Gamma 分布的前提下，得到的错误概率 P 为

$$\begin{aligned}P(T)&=P(R<T\,|\,\text{同一均匀区})\\&=\int_0^T f(R\,|\,1)\mathrm{d}R\\&=\int_0^T\frac{\Gamma(2NL)}{\left(\Gamma(NL)\right)^2}R^{NL-1}\frac{2}{(R+1)^{2NL}}\mathrm{d}R\end{aligned} \tag{3}$$

用 Ratio 算法做 4 个方向检测时，如果忽略 4 次检测事件的相关性，可以将 4 个不同方向的检测过程认为是 4 重伯努利(Bemoulli)实验，又 $P_1\in[0,1]$，检测过程满足几何分布，此时 4 个方向检测时的错误概率为

$$P_4=1-(1-P_1)^4 \tag{4}$$

由式(3)，式(4)，以图像视数 L=3 为例，可得出错误概率曲线如图 2。

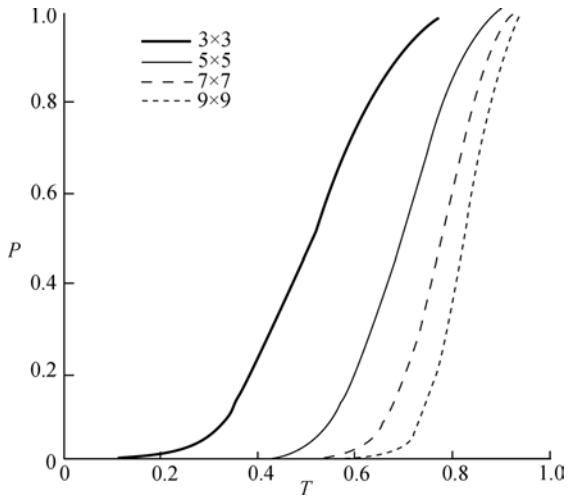

图 2 4 个方向检测时，P-T 曲线

Ratio 算法的错误概率仅由 SAR 图像视数 L、阈值 T、检测窗内个区域的像元数 N 决定，不依赖于像元灰度值，故可以克服灰度不均匀的问题，同时对于 SAR 的斑点噪声也有比较好的抑制效果，是具有恒虚警率的边缘检测。Ratio 算法具有很好的 SAR 图像边缘分析能力，但是当检测窗口越大时，边缘展宽问题越严重，若要获取单像元的边缘，则还需要进行一些处理。我们的目的只是通过边缘图得出溢油的大概位置并划分 AOI 区域，对边缘的精确度要求并不是很高，ROA 检测的结果可以直接进行下一步的 AOI 提取，大大简化了算法，缩短了计算时间。

2.2.2 AOI 提取

经过边缘检测，获得二值化边缘信息图，进行自动 AOI 的选取。将边缘图进行连通区域的变换并去除过于细小的连通区域，对每个连通区域进行加框以形成最初的 AOI。

在 SAR 溢油图像中，除了油膜和海水之外，还会存在一些岛屿和船只等对象，在边缘信息图中也包含了这些对象的边缘，故在初始 AOI 中，包含的可能不是我们需要提取的溢油，而是灰度相对比较亮的岛屿和船只，这将会影响后面的溢油提取效果，增加虚警率。因此，在作进一步的处理前，有必要对这些 AOI 进行滤除。

我们采取一种基于区域生长的方法对所有的 AOI 进行预处理。流程如下:

(1) 对于某个 AOI，选择一个灰度阈值。

(2) 寻找 AOI 中第一个大于该阈值的未标记像元点，如果找到，进栈，并对该像元作标记，统计值 Count=1，否则，跳出当前处理，转入下一个 AOI。

(3) 检测栈是否为空，若不为空，则将栈内第一个像元出栈，并对其进行 4 连通区域的检测，将大于阈值的未标记邻域像元入栈，将入栈像元进行标记，并将 Count 值加 1。若栈为空，转入(2)。

(4) 若 Count>area/5，area 为 AOI 的面积，则删除该 AOI，转入对下一个 AOI 的处理，否则转入(3)。

经过上一步的处理后，所获得的 AOI 便包含了大部分的溢油信息。把所有 AOI 的边框向四周扩大，以增加背景信息，同时将相隔比较近的 AOI 进行合并，获得最终的 AOI。

2.3 改进的 CFAR 检测

恒虚警率(CFAR)监测是雷达自动目标检测的一个重要组成部分，它的实质是针对不同背景来调整虚警概率到指定的等级。CFAR 检测技术的关键是确定自适应阈值，假设 $p(x)$为雷达杂波分布模型的概率密度函数，令 $F(x)=\int_0^x p(t)\mathrm{d}t$，可见，$F(x)$是递增函数，通过求解方程

$$1-P_{\mathrm{fa}}=\int_0^{I_c} p(x)\mathrm{d}x \tag{5}$$

可以得到阈值 I_c，其中 P_{fa} 为虚警概率。

对于给定的 P_{fa}，可以通过二分法近似地得到式(5)的解。寻找一个正整数，满足

$$F(I)\leqslant 1-P_{\mathrm{fa}} \quad 且 \quad F(I+1)>1-P_{\mathrm{fa}} \tag{6}$$

则此时的 I 就为阈值 I_c。

由式(5)可知，对杂波背景的分布模型进行估计，是 CFAR 检测的基础，也是降低虚警，不丢失目标的关键。一般认为，以海洋为背景的杂波通常服从 K 分布和 Weibull 分布模型。但是由于溢油信息比海面的灰度值低，在进行 CFAR 检测之前，需要将图像进行反转，反转后的图像其灰度集中在灰度值较高部分，与反转前的图像的杂波模型存在较大差异。本文通过实验，选取 Weibull 分布作为杂波模型。

韦布尔分布的概率密度函数表示为

$$p(x)=\begin{cases}\dfrac{c}{b}\left(\dfrac{x}{b}\right)^{c-1}\exp\left[-\left(\dfrac{x}{b}\right)^{c}\right], x\geqslant 0\\ 0, x<0\end{cases} \tag{7}$$

式中，参数 b 为尺度参数，c 为形状参数。当 c=2 时，Weibull 分布蜕化为 Rayleigh 分布，当 c=1 时，Weibull 分布蜕化为指数分布。

利用上述杂波模型，对于每一个 AOI 定义一个局部窗口，这样每个 AOI 就被划分为保护部分和背景部分(图 3)。背景窗口用于背景杂波统计，从而计算出目标检测阈值，使用保护窗口的目的是为了防止目标像元泄露到背景窗口而影响背景杂波统计的正确性。保护窗口的尺寸根据经验选择，本算法将其长宽设为 AOI 长宽的 3/5。

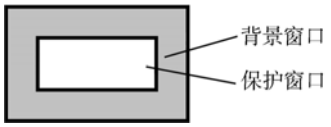

图 3 窗口结构

根据背景窗口的数据，利用 Weibull 分布的性质，可以通过 Weibull 分布的一阶矩和二阶矩的相互关系求得 Weibull 分布的尺度参数和形状参数。

Weibull 分布的一阶矩和二阶矩分别为:

$$E[x]=\int_{-\infty}^{+\infty} xP(x)\mathrm{d}x=b\Gamma\left(1+\frac{1}{c}\right) \tag{8}$$

$$E[x^2]=\int_{-\infty}^{+\infty} x^2P(x)\mathrm{d}x=b^2\Gamma\left(1+\frac{2}{c}\right) \tag{9}$$

定义

$$R=\frac{E[x^2]}{(E[x])^2}=\frac{\Gamma\left(1+\frac{2}{c}\right)}{\left[\Gamma\left(1+\frac{1}{c}\right)\right]^2} \tag{10}$$

上式的一个最佳的多项式曲线拟合为 $c=\frac{a_2}{R-1}+\frac{a_1}{\sqrt{R-1}}+a_0$，其中参数 $a_2=0.0791, a_1=0.8481, a_0=0.0817$。

从而 Weibull 分布的尺度参数 $b=\frac{E[x]}{\Gamma\left(1+\frac{1}{c}\right)}$，根据 b、c 的值，代入式(6)和式(7)，即可求出阈值。

2.4 检测后结果处理

在目标的检测上采用的算法是 CFAR 检测，而该算法存在的不足之处就是检测是针对像元来进行的，SAR 图像存在斑点噪声，使得监测出来的目标有可能为多连通区域，另外，监测出来的溢油区域边缘细碎部分过多，会导致检测出来的周长偏长。为了提高溢油检测的准确性，有必要对检测结果进行后期处理，从而获取更加精确真实的信息。本文主要采用形态学和边界跟踪等算法进行后处理。

3 试验结果分析

综合应用上述方法，我们对渤海地区的溢油图像进行了初步的试验研究。实验所采用的图像均为 Envisat 渤海区域图像，考虑到全局背景和局部背景可能存在分布差异，在虚警率的选取上，对于不同的算法，通过实验对比，来确定最佳虚警率，以获得理想的计算结果。

图 4(a)溢油图像大小为 4560×4128，获取时间为 2007 年 1 月。可以看见海面受风力或其他因素的影响，在图像上形成了鱼鳞状波纹，而且，由于侧视成像的影响，整幅图像的灰度已经呈现出了不均匀分布。

全局 CFAR 检测结果如图 4(b)。实验表明，当虚警率为 0.03 时，检测结果相对比较理想，但是由于采用的是全局阈值，使得图像中央灰度偏暗的波浪也被检测成溢油，监测出的虚警比较多，而原图像中用矩形框标识出来的那部分线性溢油相反却没有完整被检测出来。

图 4(c)是经过本文算法得出的结果，ROA 边缘检测中窗口大小选为 9×9，由于图像中波浪部分灰度变换较缓慢，若将掩模窗口取值过大，会导致波浪区域也检测为 AOI，故将掩模区域取为 3×3，即在目标像元 4 个方向均设置一个掩模像元。其中的 CFAR 检测部分虚警率取为 0.02，矩形方框是算法自动选取的 AOI 区域。可以看出，对于图像中的大部分溢油能有效地检测出来，同时还有效的抑制了海面波浪对于检测带来的负面影响。

图 5(a)是另一幅溢油图像，图像大小 1364×1404，获取时间为 2007 年 9 月，可以清楚的看见图像中存在不少灰度较高的船只，同时整幅图像的灰度也表现出了不均衡。对该图像分别采用全局 CFAR 检测和文本的算法，前者虚警率设为 0.1，后者为 0.12，所得结果分别如图 5(b)，(c)所示。对比可以发现，本文的算法很好的将图像左下角的溢油检测了出来，且有效的抑制了船只在边缘检测中带来的影响。

图 6(a)和 6(b)分别是未加保护窗的 CFAR 检测结果和本文所用的加保护窗 CFAR 检测，在虚警率取相同值(0.12)的情况下，图 6(b)中检测的效果明显比图 6(a)要好，说明改进的 CFAR 算法能够更好的匹配该杂波模型。图 6(c)是经过后处理所得到的最终边缘值，与图 6(b)的边缘相比，经过后处理后，使得溢油的边缘更加平滑，边界细碎部分得到了很好的抑制。

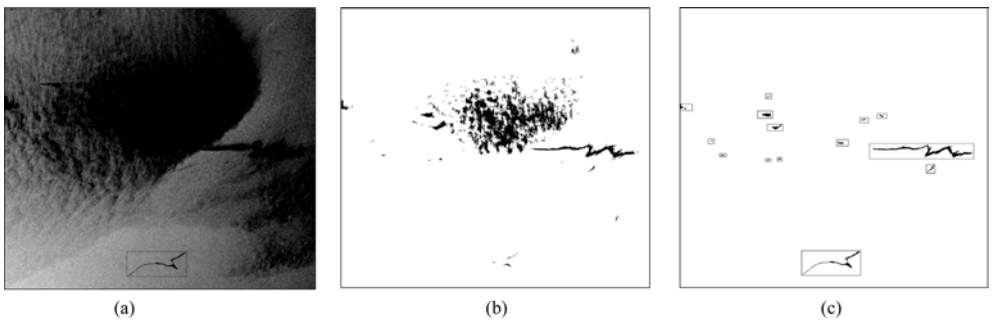

图 4 渤海区域 Envisat 溢油图像及检测结果

(a)原始图像; (b)全局 CFAR 检测的结果; (c)本文算法检测结果

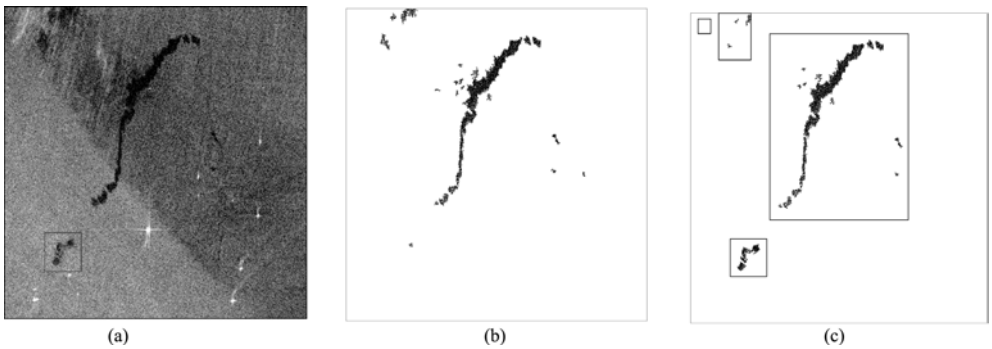

图 5 渤海区域 Envisat 溢油图像及检测结果
(a)原始图像; (b) 全局检测结果(虚警率 0.1); (c) 本文算法检测结果

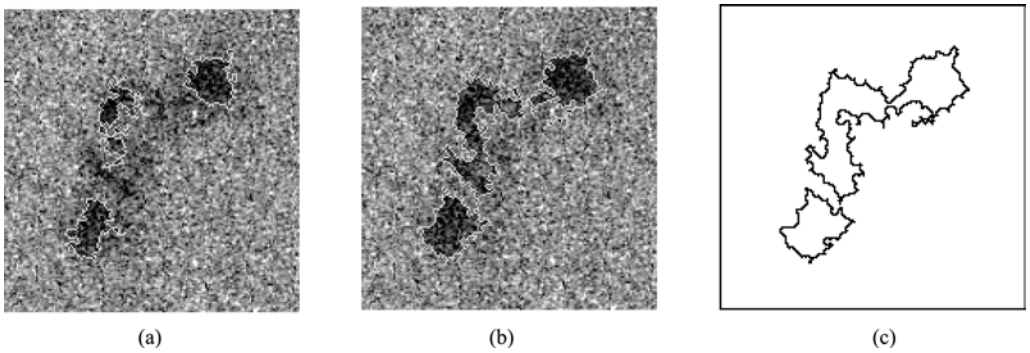

图 6 改进的 CFAR 检测及后处理结果
(a) 未加保护窗; (b) 加保护窗; (c)后处理结果

通过采用不同区域多景 SAR 图像进行算法验证, 证明本算法具有较高的可靠性, 在实际应用中能够取得较为理想的结果。

4 结 论

在本文中, 通过对 SAR 溢油图像的分析, 提出一种基于边缘检测的溢油提取算法。实验结果证明: 对于灰度不均匀的图像, 本文提出的算法明显要优于一般的全局检测, 能有效的检测出目标区域, 降低虚警。同时由于首先对 AOI 进行检测, 凸显出目标所在区域, 在对大图像的处理上具有更高的时效性, 提高了检测精度, 并且易于实现。当然本算法也存在一些不足之处, 比如所有的 AOI 难以满足同一个杂波模型和虚警率等, 这些问题还有待进一步改进。

REFERENCES

Araujo R T S, Medeiros F N S, Costa R C S, Marques R C P, Moreira R B and Silva J L. 2004. Spots segmentation in SAR images for remote sensing of environment. *IEEE Image Analysis and Interpretation*. 95—99

Barni M, Betti M and Mecocci A. 1995. A fuzzy approach to oil spill detection on SAR images. Proc.IGARSS '95. **1**: 157—159

Bjerde K W, Solberg A H S and Solberg R.1993.Oil spill detection in SAR imagery. Proc. IGARSS'93. **3**: 943—945

Chang L, Cheng C M and Tang Z S. 2005. An automatic detection of oil spill in SAR images by using image segmentation approach. Proc. IGARSS'93. 1021—1024

Ganugapati S S and Moloney C R. 1995. A ratio edge detector for speckled images based on maximum strength edge pruning. *IEEE Image Processing*, **2**: 165—168

Li L, Deng F, Peng H L. 2002. CFAR target detection in SAR imagery. *Journal of Test and Measurement Technology*, **16**: 9—13

Lu Y, Sun H, Cao Y F, Wang Q and Xu G. 2003. An improved edge detection algorithm of SAR Images. *Journal of Wuhan University*, **49**(1): 107—111

Migliaccio M, Tranfaglia M and Ermakov S A. 2005. A physical approach for the observation of oil spills in SAR images. *IEEE Journal of Oceanic Engineering*, **30**: 496—507

附中文参考文献

李岚, 邓峰, 彭海良. 2002. 合成孔径雷达图像的恒虚警率目标检测. 华北工学院测试技术学报, **16**: 9—13

吕毅, 孙洪, 曹永峰, 王青, 徐戈. 2003. 一种改进的 SAR 图像边缘检测方法. 武汉大学学报, **49**(1): 107—111